THE ROLE OF GRAIN BOUNDARY ORIENTATION AND SECONDARY PHASES IN CREEP CAVITY NUCLEATION OF A 316H BOILER HEADER

Tomas L. Martin[1], Siqi He[1], Alexander D. Warren[1], Hao Shang[1], David M. Knowles[2,3], Peter E.J. Flewitt[1]

[1]H.H. Wills Physics Laboratory, University of Bristol, Bristol, UK
[2]Henry Royce Institute, University of Manchester, Manchester, UK
[3]Faculty of Engineering, University of Bristol, Bristol, UK

ABSTRACT

Cavity formation during creep of steels at high temperatures and stresses is closely related to the original and evolved microstructure, particularly the orientation between grains and precipitation at the grain boundaries. Understanding the initiation, growth and coalescence of creep cavities is critical to determining the operational life of components in high temperature, high stress environments such as an advanced gas-cooled nuclear reactor. However, accelerated laboratory-based testing frequently shows another kind of void within the microstructure, caused by plastic damage and ductile failure, particularly if a specimen fails during a test. This paper compares the type of voids and cavities observed in an AISI 316 stainless steel after extensive service in a gas-cooled nuclear reactor boiler header and after uniaxial creep testing of a similar material at higher stresses. The differences between the features observed and their potential mechanistic origins are discussed.

Keywords: Creep, cavitation, plastic deformation, voids

1. INTRODUCTION

Voids and/or cavities are frequently formed within creep test specimens where the test conditions are accelerated to provide data included in long-term component assessments. These defects often nucleate at secondary phase precipitates both within the grain structure and particularly at grain boundaries. The nucleation, growth and coalescence of both voids due to plastic deformation at higher stresses [1], and cavities due to creep deformation [2,3,4], typically at lower stresses and higher temperatures have been documented extensively in a range of steels used for service components.

When investigating the structural integrity of a material exposed to creep during extended service life of a component in a high temperature application such as the boiler of an advanced gas-cooled nuclear reactor (AGR), the initiation and growth of creep cavities is a key part of the failure mechanism, and cavities are frequently observed at key locations such as weldments of components where stress is locally accumulated. However, analyzing ex-service specimens from such components can be challenging -firstly, the cost of retrieving specimens from plant during operation can be high, and secondly the material removed can only be investigated after the time at which it was removed from service. This may mean cavitation is already fairly advanced, and understanding the causes behind the initiation of cavities at this stage can be challenging.

To investigate early stages of creep cavity formation, typically simulated tests are performed in the laboratory, often using a tensile specimen under accelerated stresses and/or temperatures. Generally, these tests are at stresses substantially higher than experienced in plant in order to produce data within a reasonable time frame. However, performing such higher stress testing can result in void formation due to plastic deformation in addition to any creep cavities. In addition, the conditions for early formation is also a function of stress state. Lonsdale and Flewitt demonstrated the change from grain boundary cavitation to plastic voids is a function of the relative contributions of maximum principal and equivalent stresses [5]. In particular, if a specimen has failed during an accelerated test, extensive plastic damage can obscure and confuse analysis of any creep cavitation at grain boundaries.

When performing microscopy on such specimens, it is important that the differing mechanisms for voids and cavities are understood, and that the difference in size, geometry and location is documented, so that the two mechanisms can be distinguished. In this paper, we will present examples of cavity/void formation observed in an AISI 316 stainless steel under both ex-service conditions and accelerated uniaxial laboratory creep tests, and compare the observed microstructures.

1.1 Failure mechanisms in ductile materials

Ductile alloys fail typically due to the nucleation, growth and coalescence of voids. Under hydrostatic tensile stress, spherical-shaped voids nucleate at inclusions and secondary phase precipitates, which will continue to grow if applied stress remains. Eventually, voids become sufficiently large enough to coalesce with other voids, leading to cracking and eventual failure [6]. In plastic deformation at low temperature, voids nucleate at regions of inhomogenous stress – typically the interface between particles and the matrix, or within larger inclusions [7].

Creep fracture also occurs by nucleation and growth of diffusive cavities and subsequent coalescence into cracks. This

[1] Contact author: tomas.martin@bristol.ac.uk

can also be linked with a small (≤10%) decrease in cross-section due to large strain, thermal coarsening of precipitates and/or environmental degradation [8]. Three principle mechanisms are proposed for cavity nucleation: grain boundary sliding [9], dislocation pile-up [10], and condensation of atomic vacancies [11], although it is still unclear which is the dominant nucleation mechanism [12]. Subsequent growth is typically by vacancy diffusion.

The challenge, however, when studying the microstructure of materials creep tested in the laboratory, is how to distinguish between a diffusive creep cavity and a purely plastic void, as a lot of the mechanisms behind the formation are shared. Creep is typically defined as time-dependent plasticity at a fixed stress at elevated temperature of 50% of the melting temperature or above, whereas at lower temperatures plasticity is not expected at such low fixed-rate stresses [13].

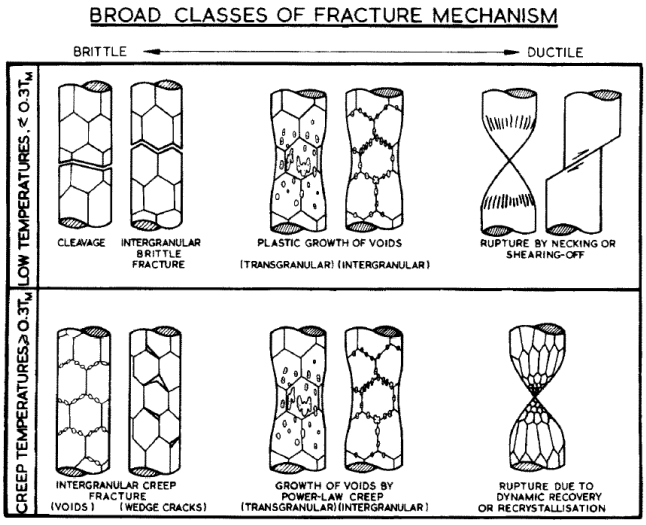

FIGURE 1: CLASSIFICATION OF FRACTURE MECHANISMS AT DIFFERENT DUCTILITY FOR FCC MATERIALS AT LOW TEMPERATURE (TOP ROW) AND HIGH TEMPERATURE (BOTTOM ROW). [14]

Past work by Ashby *et al* [14, 15] explored the use of deformation-mechanism maps which detailed the theoretical deformation mechanisms that could be experienced by a crystalline metal depending on the stress experienced. This was split into two broad classes of fracture mechanism depending on whether the temperature was above or below $0.3M_T$, where M_T is the melting temperature of the material, as shown in Figure 1. At low temperatures $<0.3M_T$, failure can occur by cleavage or intergranular brittle failure, plastic growth of voids, or rupture by necking, in order of increasing ductility. At higher temperatures $>0.3M_T$, brittle materials generally fail by intergranular creep fracture through initiation of void or wedge cracks, medium ductility samples fail through growth of voids by power-law creep, and finally the most ductile materials rupture due to dynamic recovery or recrystallisation. Frost and Ashby later created the concept of a deformation mechanism map that showed the type of deformation expected at different combinations of normalized shear stress and temperature, as pictured in Figure 2 for type 316 steel with an average grain size of 50μm. [16] Although these mechanism maps are generalized, they can help to understand the transition between diffusional flow at lower stresses towards dislocation flow (also called power-law creep), at moderate stresses and elevated temperatures, moving into dislocation glide (plasticity) at very high stresses.

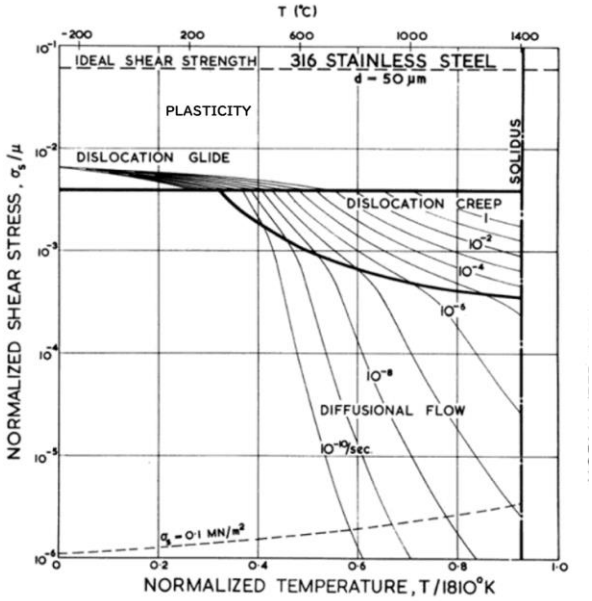

FIGURE 2: ASHBY-FROST DEFORMATION MECHANISM MAP FOR A TYPE 316 AUSTENITIC STAINLESS STEEL WITH AN AVERAGE GRAIN SIZE OF 50μM. [16]

The difference between ductile failure at low temperature through plastic growth of voids and the growth of voids by power-law creep is not so well understood, at least at the initiation stage. In both mechanisms, voids nucleate at inclusions due to a concentration of stress at the interface between inclusion and matrix. Once the stress reaches a critical value this leads to either a breaking of the inclusion or a void nucleation, which under further stress can grow and coalesce. As these voids themselves will enhance stress locally, they can accelerate damage in the surrounding region until a material ruptures at that point.

At higher temperatures and high stresses, the failure mechanism of medium ductility specimens is very similar to that at low temperature – voids nucleate at inclusions, coalescing with increasing stress until fracture occurs. However, at higher temperatures and lower stresses, matter can diffuse between regions on the surface of an inclusion, leading to creep damage at steady state stresses lower than the critical stress for plastic deformation at ambient temperatures. As the formation of cavities can occur due to creep at elevated temperatures and due to plasticity at high stresses, it is important to study the way these features occur within the microstructure of a material and understand whether the position and appearance of voids and cavities differs between the two regimes.

Often, laboratory-based tests use higher stresses to accelerate creep, but this can potentially move the material into the plastic regime, particularly during initial loading. When such a specimen fails, extensive plastic damage during tertiary creep can obscure initial cavity formation through sudden coalescence and growth of ductile voids. If progress is to be made on establishing the mechanism behind initiation of creep, it is vital that the damage caused by this plasticity can be distinguished from the initial diffusive creep cavity formation. In the results shown in this article, we show microscopy of voids experienced by a 316H steel under different stresses to explore the nature of creep cavitation and ask – if a cavity can be formed by both long-term creep behavior and high temperature ductile deformation, how do we distinguish between these mechanisms?

2. MATERIALS AND METHODS

The material used throughout this work was 316H steel, taken from boiler headers that had been in service in an advanced gas-cooled nuclear reactor operating at temperatures in the range between 480-530°C for 50,000-65,000 hours. The nominal composition of the material in wt.% was 17.17% Cr, 11.83% Ni, 2.19% Mo 1.98% Mn, 0.4% Si, 0.1% Co, 0.06% C, 0.021% P, 0.014% S, 0.005% with a balance of 66.23% Fe. Following removal from plant, the header was sectioned into test specimens and subjected to additional testing, as detailed in Table 1.

Specimen	Post-service test	Temperature of test	Stress	Test duration (hours)
1	Ex-service only	480-550°C (in-service condition)	Complex	50,000-65,000 hours (in-service condition)
2	Strain controlled creep test	550°C	440MPa	1500
3	Creep relaxation	550°C	390MPa	1511

TABLE 1: SUMMARY OF THE SPECIMENS COMPARED WITHIN THIS WORK

The first specimen removed from service after 65,000 hours had no post-service heat treatment or mechanical testing, and was imaged directly from the sectioned material. The material was cut from a region of material close to a weld in the boiler header, and as such residual multi-axial stresses are expected, although due to the complex nature of stresses in an ex-service component it is challenging to specify the exact stress experienced. Specimens 2 and 3 were cut into notched hourglass tensile test specimens before uniaxial creep testing. Specimen 2 underwent a strain-controlled creep test at 550°C and 440MPa, failing on reloading after 1500 hours, whilst specimen 3 failed after 1511 hours in uniaxial creep relaxation with a temperature of 550°C and an applied stress of 390MPa.

Tensile specimens were sectioned lengthways and the ex-service material was cut into smaller sections. Specimens were polished using SiC pads of decreasing grit size followed by diamond pastes of 3µm, 1µm, 0.25µm and 0.1µm, with a final finish prepared using vibropolishing in a suspension of colloidal silica particles for 5-8 hours [17].

The polished specimens were imaged in scanning electron microscope (SEM) using a Zeiss SigmaHD field-emission SEM. In addition, specimens were imaged using the focused ion beam (FIB) of an FEI Helios Dualbeam FIB instrument. To provide contrast between phases, the surface was imaged using an ion beam at 30kV and 90pA whilst a flow of xenon difluoride gas was passed across the surface using a gas injection system. This has previously shown to be able to distinguish between carbides, ferrite and austenite in steels [18]. To observe the three-dimensional shape and distribution of cavities, samples were cross sectioned using the Dualbeam FIB [19]. A protective layer of platinum was deposited using the gas injection system before slices of 1µm were removed at 30V and 6.5nA, with the FEI automated slice and view software taking an image using the secondary electron detector after each slice. Following completion of the FIB sectioning, the SE images were reconstructed into a 3D volume using the Thermo-Fisher Avizo 3D visualization and analysis software package.

3. RESULTS AND DISCUSSION

3.1 Creep Cavitation in ex-service steels

Figure 3(a) shows the damage observed in the ex-service specimen without any additional heat treatments of mechanical testing. Within a few mm of the weld metal, extensive cavitation is observed along grain boundaries, with a mean diameter of 0.7-0.9µm and an irregular polyhedral shape. As the shape of the header was complex, the direction of the stress axis is not known for this specimen, unlike the uniaxial specimens.

The XeF_2-enhanced focused ion beam image in Figure 3(b) shows the typical microstructure at the grain boundaries. Cavities are always co-located with both $M_{23}C_6$ carbide and bcc phase precipitates at the boundaries. The bcc phase has been identified using transmission electron microscopy diffraction as ferrite in a separate work. [20]

Figure 3(c) shows the 3-dimensional distribution of cavities along a grain boundary using FIB cross-sectioning and 3D image reconstruction. The size and shape of the cavities is similar to that observed on the surface, showing that the surface preparation is not significantly changing the cavities being sectioned. The overall conclusion from the ex-service material is that the individual cavities are isolated from each other, and show limited evidence of coalescence beyond a few µm. They are not present along every grain boundary, but when present, damage is extensive but regular in distribution.

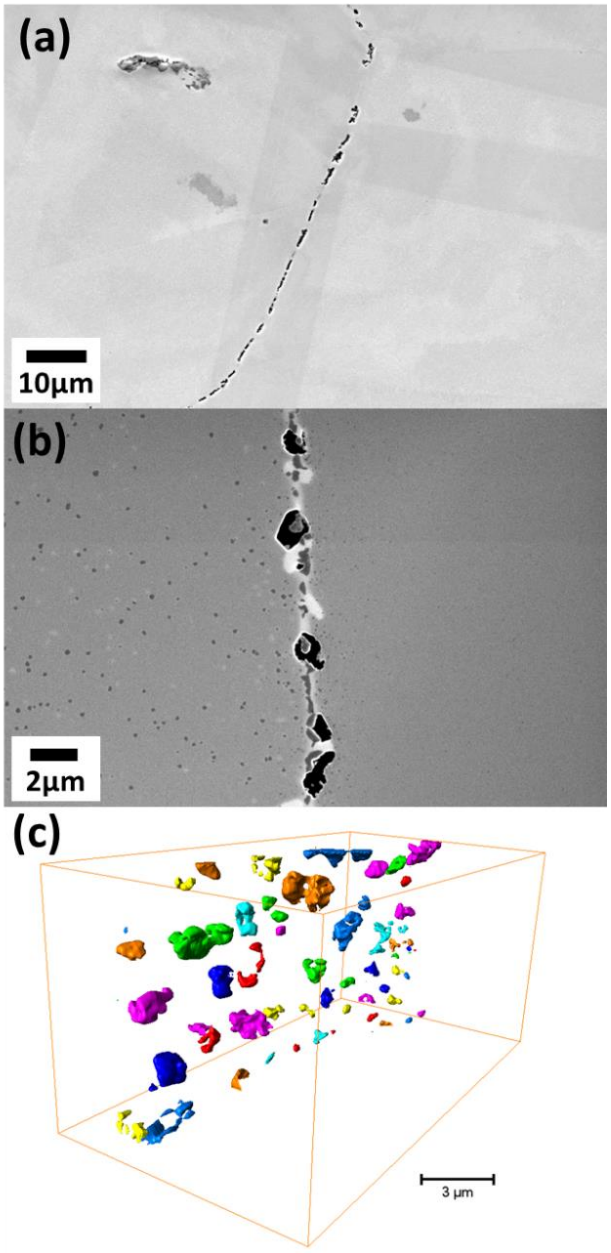

FIGURE 3: DAMAGE CLOSE TO A WELD IN A 316H BOILER HEADER AFTER 65,000 HOURS IN SERVICE AT 490-530°C. (A) SCANNING ELECTRON MICROGRAPH SHOWING A GRAIN BOUNDARY DECORATED WITH ISOLATED CAVITIES, (B) XEF_2-ENHANCED FOCUSED ION BEAM IMAGE SHOWING THE RELATIONSHIP BETWEEN CAVITATIES (BLACK), CARBIDES (DARK GREY) AND FERRITE (WHITE) AT A BOUNDARY, (C) 3-DIMENSIONAL RECONSTRUCTION OF FOCUSED ION BEAM SLICE AND VIEW SHOWING THAT CAVITIES CONTINUE AT GRAIN BOUNDARIES WITHIN THE MATERIAL VOLUME.

3.2 Damage observed after post-service accelerated uniaxial creep testing

Figure 4 shows SEM micrographs of 316H boiler header material that has undergone a strain-controlled creep tests in a tensile test rig. The specimen failed on reloading after 1511 hours at 550°C and 390 MPa. The images in Figure 4 are taken across a cross-section of the tensile test specimen within the first few mm below the notch where rupture occurred.

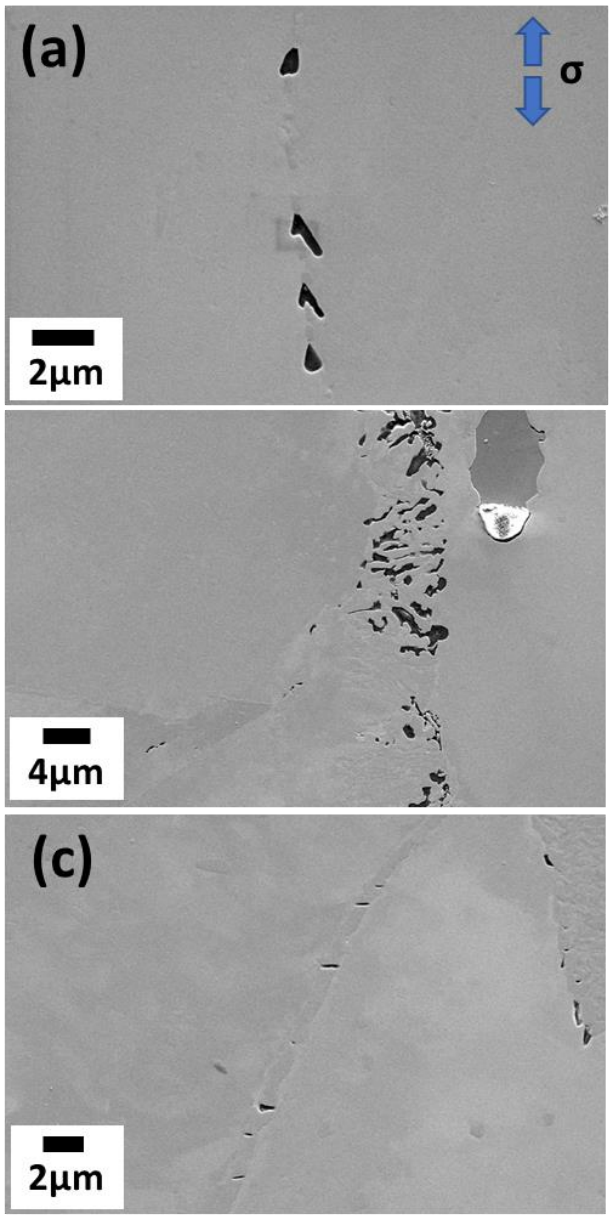

FIGURE 4: DAMAGE IN A 316H BOILER HEADER AFTER TESTING UNDER STRAIN-CONTROLLED CREEP CONDITIONS IN A TENSILE TEST RIG AT 550°C, AND 390MPA FOR 1511 HOURS. (A) FACETED CAVITIES ON AN INCLINED GRAIN BOUNDARY, (B) CAVITATION AT A REGION OF RETAINED FERRITE AND (C) PRECIPITATE BREAKING ALONG GRAIN BOUNDARIES PERPENDICULAR TO THE STRESS DIRECTION. THE TENSILE STRESS DIRECTION IS INDICATED BY THE ARROWS IN (A).

Whilst cavities are also visible in this specimen at grain boundaries, the morphology is different to that observed in the

ex-service specimen. Figure 4(a) shows a series of faceted cavities characteristic of those observed in this specimen, with sharper and more delineated edges than the cavities shown in Figure 3, and less irregular shapes. These features were not observed in material prior to testing. The cavities are often oriented in a parallel direction to each other, and in this case the two central cavities in Figure 4(a) are both oriented with their longest edge roughly 45° from the tensile stress direction indicated by the arrows at the top right of the figure. This may indicate that the cavities are forming along the highest shear stress according to the Schmid factor – perhaps suggesting a more purely plastic behavior. However, this limited set of data can only suggest such behavior, and a more comprehensive study is required and combined with relevant modelling before the mechanism can be fully documented.

Figure 4(b) and (c) show other forms of damage common in this specimen – (b) shows extensive damage at a region common in this material containing ferrite retained during casting. There are many cavities associated with these regions, which has also been observed in the material in its pure ex-service state. It is possible that some of these cavities existed at a much smaller scale prior to the uniaxial test and have grown and coalesced during the test, but as the specimen has experienced so much damage during rupture it is difficult to be certain. The damage observed at these retained casting regions in the ex-service specimen was much less extensive.

Finally, Figure 4(c) shows a feature commonly observed on the uniaxial creep specimen but not in the ex-service material – that of grain boundary precipitate-interface separation, with very thin cavities perpendicular to the stress direction. Again, this is very indicative of a plastic deformation-driven failure rather than a diffusion process, strongly suggesting that stress rather than temperature is driving the formation of these features.

Figure 5 shows SEM micrographs from a second specimen, in this case subjected to a uniaxial creep relaxation test at 550°C and 440MPa, failing after 1500 hours. Notable in the microstructure here is even more extensive coalescence of damage, as might be expected from a test at higher stresses than the previous specimen.

Figure 5(a) shows a grain boundary perpendicular to the stress direction with extensive damage across the majority of the boundary, approaching a separation of the two austenitic grains leaving the grain boundary inclusions virtually unconnected from the parent matrix. This is strongly indicative of plastic void growth, with either substantial coalescence of earlier independent cavities, or a faster delamination of the two sides of the grain boundary.

Figure 5(b) shows a lower magnification image of the material, with again substantial cavitation concentrated at a region of retained ferrite at the bottom right of the image. The damage appears even heavier than that of Figure 3(c), with a large proportion of the retained region missing. This could be due to cavitation, but as the precipitates being so unconnected to the material they could be lost more easily during specimen preparation.

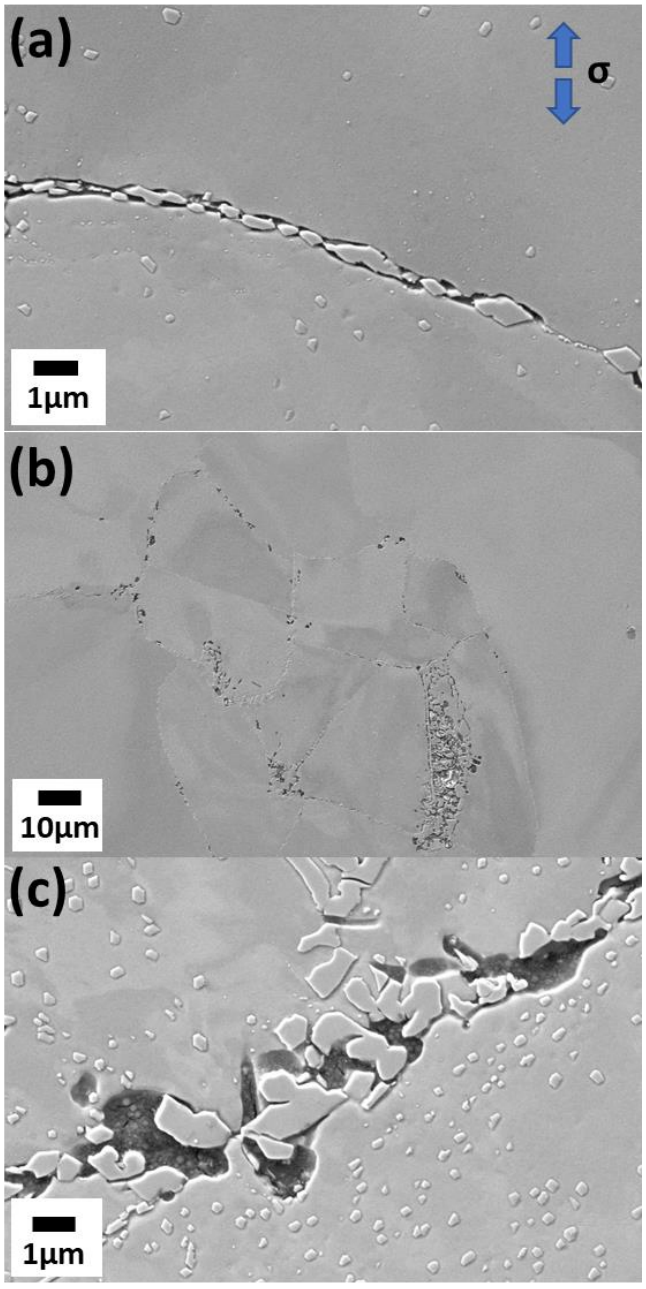

FIGURE 5: 316H BOILER HEADER AFTER TESTING UNDER UNIAXIAL CREEP RELAXATION CONDITIONS AT 550°C, AND 440MPA FOR 1500 HOURS. (A) SHOWS SEPARATION OF AN ENTIRE GRAIN BOUNDARY AROUND MULTIPLE PRECIPITATES (B) SHOWS CAVITATION AT A REGION OF RETAINED FERRITE AND (C) SHOWS PRECIPITATE BREAKING ALONG GRAIN BOUNDARIES, WITH A ROUGH SURFACE TO THE CAVITIES INDICATING THAT OXIDATION MAY HAVE OCCURRED. THE TENSILE STRESS DIRECTION IS INDICATED BY THE ARROWS IN (A).

Figure 5(c) shows a higher magnification image of a boundary where again, extensive cavities are observed around grain boundary precipitates, likely to be carbides. Of interest here is the rough surfaces of the cavities, which appear as if some oxidation may have occurred during the test.

Comparing the three specimens in this paper, it is clear to see that as the stress experienced by the specimen increases, using microscopy to characterize cavitation becomes more challenging. Specimens of AISI Type 316H steel after extended service at 480-530°C showed small, irregular polyhedral shaped cavities at grain boundaries, with little evidence of coalescence beyond a few μm.

After similar material was tested using several high temperature uniaxial creep tests, cavitation was still observed at grain boundaries within the first few mm of the rupture notch, however the types of cavity identified in electron microscopy were noticeably different, with more angular, faceted cavities, precipitate breaking and notably more extended and connected cavity networks, particular at higher applied stresses, where grain boundaries were extremely separated, and retained ferrite regions were highly damaged.

Understanding the initiation of these cavities is very challenging as the act of rupture in the accelerated test specimens will have obscured much of the evidence of the initiation of cavities, and plastic deformation dominates the microstructure after the tertiary stage of failure. The data presented here are only a small selection of conditions and microstructures required to understand the full mechanistic behavior of cavity initiation in creep conditions. Initiation of creep cavities is very complex system to model, particularly for ex-service specimens where long-term thermal ageing can contribute and stress states are more complex than for uniaxial tests. However, the results presented here do highlight the important role that plasticity plays within these initiation mechanisms and that the role of plastic deformation should be considered, particularly for higher stress laboratory testing. Future work in this area will explore in more detail the relationship between grain boundary phase evolution, orientation and cavity nucleation at different stresses and temperature to develop a fuller understanding of this important degradation mechanism [20].

4. CONCLUSION

Whilst the mechanisms of creep and plastic deformation are well understood within the growth regime, the initial nucleation of cavities share several closely linked mechanisms and can be challenging to distinguish by a range of imaging techniques. This is particularly important in laboratory-based accelerated creep tests, where plasticity can play an important role due to the higher stresses used to accelerate the test. A comparison of a long-term ex-service AISI 316H steel specimen shows that creep during service creates cavities along grain boundaries that are various rounded and irregular polyhedral shapes, with little coalescence. Accelerated tests of the same material show more angular and faceted cavities, as well as precipitate-interface separation and coalescence of cavities at retained ferrite regions and increasingly along entire boundaries at higher stresses, indicating a higher proportion of plastic damage. To ensure accurate identification of the early stages of creep, it is important to interrupt the specimens early in the creep life. This can prevent the extreme damage at the end of a test from obscuring smaller cavities that might provide insight into the nucleation process. The microscopy presented here is not a comprehensive overview of the range of conditions that might produce cavitation at boundaries, and there still remains substantial additional work to document creep cavitation behavior even in this single material before a true mechanistic understanding of nucleation can be fully developed.

ACKNOWLEDGEMENTS

Dr Mike Spindler and EDF Energy are thanked for providing the 316H material and performing the strain-controlled creep test (specimen 2). Edward Hares and Mahmoud Mostafavi are thanked for performing the creep relaxation test for specimen 3. This work was supported by the EDF High Temperature Centre and ESPRC grant EP/R026076/1.

REFERENCES

[1] Tai, W. H. *Plastic damage and ductile fracture in mild steels*, Engineering Fracture Mechanics 37, 4 pp. 853-880 (1990)

[2] Turski, M., Bouchard, P.J., Steuwer, A. and Withers, P.J. *Residual stress driven creep cracking in AISI Type 316 stainless steel*, Acta Materialia, 56, 14, pp. 3598-3612 (2008)

[3] Slater, T.J.A., Bradley, R.S., Bertali, G., Geurts, R., Northover, S.M., Burke, M.G., Haigh, S.J., Burnett, T.L. and Withers, P.J. *Multiscale correlative tomography: an investigation of creep cavitation in 316 stainless steel*, Scientific Reports, 7, article no: 7332 (2017)

[4] Burnett, T.L., Geurts, R., Jazaeri, H., Northover, S.M., McDonald, S.A., Haigh, S.J., Bouchard, P.J. and Withers, P.J. *Multiscale 3D analysis of creep cavities in AISI type 316 stainless steel*, Materials Science and Technology, 31, 5, pp. 522-534 (2014)

[5] D Lonsdale and P.E.J. Flewitt, *The effect of hydrostatic pressure on the uniqxial creep life of a 2¼% Cr 1% Mo steel*, Proceedings of the Royal Society, 373, 1755, (1981)

[6] Das, Arpan, Roy, Nimila and Ray, Ashok Kumar, *Stress induced creep cavity*, Materials Science and Engineering: A, 598, pp.28-33 (2014)

[7] Goods, S.H. and Brown, L.M. *The nucleation of cavities by plastic formation*, Acta Metallurgica 27 pp1-15 (1978)

[8] Ashby, M.F. and Dyson, B.F. Proc. ICF6, 3 (1984)

[9] Riedel, H. *Cavity nucleation at particles on sliding grain boundaries. A shear crack model for grain boundary sliding in creeping polycrystals*, Acta Metallurgica 32, 3, pp.313-321 (1984)

[10] Dyson, B.F., *Continuous cavity nucleation and creep fracture*, Scripta Metallurgica, 17, pp.31-37 (1983)

[11] Raj, R. and Ashby, M.F., *Intergranular fracture at elevated temperature*, Acta Metallurgica 23, pp653-666 (1975)

[12] Wen, J-F, Tu, S-T, Xuan, F-Z, Zhang, X-W and Gao, X-L, *Effects of stress level and stress state on creep ductility:*

Evaluation of different models, Journal of Materials Science & Technology, 32, 8, pp. 695-704, (2016)

[13] Kassner, M.E. and Hayes, T.A. *Creep cavitation in metals*, International Journal of Plasticity 19, 10 pp.1715-1748 (2003)

[14] Ashby, M.F., Ghandi, C. and Taplin, D.M.R. *Fracture-mechanism maps and their construction for F.C.C. Metals and Alloys*, Acta Metallurgica 27 pp 699-729 (1979)

[15] Ashby, M.F. *A first report on deformation-mechanism maps*, Acta Metallurgica, 20, pp887-897 (1972)

[16] Frost, H. and Ashby, M.F. *Deformation-mechanisms Maps*, Pergamon, Oxford, UK, (1982)

[17] A.D. Warren, A.I. Martinez-Ubeda, O.D. Payton, L. Picco and T.B. Scott, *Preparation of stainless steel surfaces for scanning probe microscopy*, Microscopy Today 24, 3, pp.52-55 (2016)

[18] A.D. Warren, P.J. Heard, P.E.J. Flewitt and T.L. Martin, *The Role of Replicated Service Atmosphere on deformation and fracture behaviour of carburised AISI Type 316H Steel*, Key Engineering Materials 827, pp. 318-323 (2020)

[19] Chen, B., Flewitt, P.E.J., Smith, D.J. and Jones, C.P. *An improved method to identify grain boundary creep cavitation in 316H austenitic stainless steel*, Ultramicroscopy 111, 5, pp.309-313 (2011)

[20] S. He, H. Shang, A.D. Warren, D. Knowles, P.E.J. Flewitt and T.L. Martin, *Microstructural observation of creep cavity formation mechanisms in ex-service AISI Type 316 Stainless Steel*, in preparation